RSC Advances

ROYAL SOCIETY OF CHEMISTRY

www.rsc.org/advances

A First principle study of H_2S adsorption and decomposition on Ge (100) surface

Tsung-Fan Teng[†,‡], *Santhanamoorthi Nachimuthu*[†], *Wei-Hsiu Hung*[‡], *Jyh-Chiang Jiang*[†*]

[†] Department of Chemical Engineering, National Taiwan University of Science and Technology, Taipei 106, Taiwan

[‡] Department of Chemistry, National Taiwan Normal University, Taipei 116, Taiwan

*Corresponding author: e-mail: jcjiang@mail.ntust.edu.tw, Phone: +886-2-27376653, Fax: +886-2-27376644**;**

Abstract

We employed density functional theory (DFT) calculation to examine the adsorption configurations and possible reaction paths for H_2S on Ge(100) surface. There are four reaction paths are proposed for the decomposition of adsorbed H_2S on Ge(100) surface and the corresponding structural conformations are studied extensively. The present study shows that two new possible products and detailed reaction mechanism for H_2S adsorption on Ge(100) surface and the results are compared with our previous study of H_2S adsorption on Si(100) surface (J. Phy. Chem. C 115, 2011, 19203). The density of states (DOS) and electron density difference (EDD) analyses are used to illustrate the interaction between S-containing species and surface Ge atoms.

Key words: H_2S, DOS, density functional theory, Ge(100).

1. Introduction

Over the past decades, high mobility semiconductors have investigated as a replacement for the Si channel due to its potential applications in high-performance metal-oxide-semiconductor (MOS) devices.[1-3] Recently, Germanium (Ge) has attracted much attention because it gives bulk electron and hole motilities at room temperature which are higher than the conventional silicon based materials.[4, 5] However, major drawbacks of the application of Ge in these devices are the poor quality of its thermal oxide compared to SiO_2 and the Ge-based MOS devices has high interface state density (D_{it}) which would result in low carrier mobility in the channel. These limitations can be overcome by the passivation of Ge surface prior to the deposition of the gate dielectric which is a key issue for semiconductor surfaces.[6, 7]

Also, the practical use of this semiconductor in the devices requires the passivation to prevent oxidation and maintain the surface order during device processing. Sulfur (S) has been shown to be one of the best passivants of semiconductor surfaces.[4] Anderson et.al., reported that the Sulfur passivation of the germanium surface via both solution and vacuum deposition techniques.[8] A sulfur adlayer is deposited on a semiconductor surface through immersion in a solution of $(NH_4)_2S$ [8] or on its exposure to elemental sulfur or H_2S.[9] On the other hand, Houssa et al. proposed two approaches for the passivation of Ge surface to promote metal-oxide-semiconductor field-effect transistor (MOSFET).[10] One of two approaches is the exposure of the Ge surface to H_2S, resulting in the formation of S-Ge bonds. Indeed, the Ge energy band gap is free of surface states after H_2S exposure, resulting in the electrical passivation of the surface, which is a crucial requirement for the potential use of Ge in the MOSFET.

Similar to Si(100) and C(100) surfaces, the reconstructed Ge(100)-2 ×1 surfaces consist of dimers connected by a strong σ-bond and a weak π-bond.[11] The diamond surface has symmetric dimers with a bond length of approximately 1.4Å, whereas the Si and Ge surfaces both have larger asymmetric, or tilted, dimers with a bond length of 2.3-2.5Å.[12-14] Distortion of the dimer bonds induces a charge transfer from the down (electrophilic) to the upper (nucleophilic) surface atom.[15] Such zwitterionic characteristics allow the surface to undergo a nucleophilic/electrophilic reaction, often with direct analogies to the molecular systems. The adsorption of sulfur on Ge(100) surface has been studied both experimentally and theoretically.[16-18]

Previously, the S-passivation on Ge(100) surface has been investigated using low-energy electron diffraction (LEED),[8, 19] high-resolution electron-energy loss spectroscopy (EELS),[20] ultraviolet photoelectron spectra (UPS),[21] X-ray photoelectron spectra (XPS),[22] temperature programmed desorption (TPD),[23] Near edge X-ray absorption fine structure (NEXAFS)[24] and multiple internal reflection-Fourier transform infrared spectrometer (MIR-IR).[25] Kuhr and Ranke [21] showed in their UPS study that, H_2S adsorbs dissociatively at 300K on a Ge surface; then decomposes completely to form sulfur at 550K. To understand the sulfidation of the Ge(100) surfaces and its possible passivating reactions, we choose H_2S as a passivant to be adsorbed on the Ge(100) surface. In this study, we report ab initio theoretical investigations to provide a complete description of the adsorption effects and thermal decompositions of H_2S on Ge(100) surface. We thereby elucidates possible mechanisms of thermal decomposition on Ge(100) that was more conformed to real surface.

2. Computational Details

DFT calculations are performed using the Vienna ab initio simulation package (VASP).[26-28] The Vanderbilt ultra-soft pseudopotential is used to describe the election-ion interactions[29] and the electron- electron exchange and correlation contributions by the generalized gradient approximation (GGA) with energy truncated at 300 eV. The Brillouin zone is sampled with Monkhorst-Pack grid, and the calculations were performed with (4×2×1) Monkhorst-Pack mesh *k*-points. We optimized the structures based on the conjugate gradient-minimization scheme taking into consideration of spin polarization. The validities of all the optimized structures and determined transition states (TSs) are checked through normal-mode frequency analysis. For a real minimum structure, all frequency must be positive; TS must have one imaginary frequency corresponding to the reaction coordinate. The clean surfaces are then modeled in the form of a slab. The c(4×2) unit cell consisted of nine atomic layers separated by a 20 Å vacuum to prevent interactions between the surface adsorbates and the preceding slab. The optimized geometry of the model Ge(100) surface considered in this study is depicted in Figure 1.

In the structural optimizations, the positions of the last three Ge layers along with the H-passivated layer on the bottom are fixed upon adsorption of H_2S and the remaining substrate atoms are allowed to relax with the adsorbates. To economize computing time, only the upper two atomic layers of the surface and adsorbate are relaxed in the vibrational frequency calculations. The adsorption energies are obtained by

$$E_{ads} = E_{Total} - (E_{Gas} + E_{Surface})$$

in which E_{Total}, E_{Gas} and $E_{Surface}$ are the respective calculated electronic energies of the adsorbed species on the surface, a gaseous molecule, and a clean surface. A negative value for E_{ads} indicates an exothermic adsorption. The relative energies (E_{rel}) are defined as

$$E_{rel} = E_{(\mathrm{LM\ or\ FS})} - E_{H_2S_{ad}}$$

in which $E_{H_2S_{ad}}$ and $E_{(\mathrm{LM\ or\ FS})}$ are the calculated adsorption energies of H_2S and local minima or final products, respectively. The nudged-elastic-band (NEB) method is applied to locate the transition state structures positioned to interpolate a series of system images between the initial and final states on the potential-energy surface.[30, 31] A spring force between adjacent images is used to maintain constant spacing between the images, and a true force is applied to impel the images into the minimum energy path (MEP), mimicking an elastic band. Each image is optimized using the NEB algorithm based on a constrained algorithm of molecular dynamics. The highest point on the MEP corresponds to a transitional structure on the proposed reaction path and its energy, relative to that of the initial state, became the activation barrier of the reaction.

The electron density difference (Q_{diff}) is calculated in a similar manner to the calculation of adsorption energy

$$Q_{diff} = Q_{A/Surf} - \left(Q_{Surf} + Q_A\right)$$

where Q_{diff} is the difference at each grid point in the total electron density matrix between that of the adsorbate-bonded surface ($Q_{A/Surf}$) and that of the sum of the surface (Q_{Surf}) and the single adsorbate molecule (Q_A). According to this definition, positive and negative values correspond to increasing and decreasing electron densities, respectively.

3. Results and Discussion

3.1. Adsorption of H_2S, HS and S on Ge(100) surfaces

To ensure the reliability of the computational method, we have calculated the lattice parameters for bulk germanium using various pseudopotentials and the values are given in Table S1 of Supplementary information. As can be seen from those values PAW-PBE and the ultrasoft pseudopotential with the generalized gradient approximation (US-GGA) gives the least discrepancy between the calculated and experimental lattice parameters among the tested pseudopotentials. In order to compare with our previous study of H_2S adsorption on Si(100) surface,[32] we considered US-GGA method for further calculations. Also, we have performed the benchmark calculations for the H2S adsorption on the clean Ge(100) surfaces with different functionals and different cutoff energy values and the calculated values are give in Table S2. It has been observed that the trends of the calculated values with different cutoff energies and functionals are almost similar and hence we have chosen the US with 300 eV cutoff energy values for our further study. Table S3 presents the comparison of calculated bond lengths and bond angles of clean Ge(100) surface with other studies[33] and it has been found that the calculated bond lengths are in agreement with the previous experimental reports.[34-36]

Previously, we found that the H_2S has three stable adsorption conformations on the Si(100) surfaces with orientation of the S-H bond;[32] similarly here we considered the same conformation of H_2S adosrbed on Ge(100) surfaces (denoted as H_2S_{ad}, H_2S_{ad}-1, and H_2S_{ad}-2) and the optimized strctures are shown in Figure 2. The calculated adsorption energies and structural parameters for different conformation of H_2S are summarized in Table 1. Among these three conformations, H_2S_{ad} is found to be the most stable with adsorption energy -0.49 eV and the other two conformations H_2S_{ad}-1 and H_2S_{ad}-2 adsorbed to the surface with adsorption energies -0.40 and -0.30 eV, respectively. From Table 1, it has been observed that the bond length of the Ge-Ge dimer is increased (~0.04 Å) and the tilting angle of Ge dimer is decreased to 16° from 20° after the adsorption of H_2S on the Ge surface, indicating the decreased zwitterionic and π-bond characters of the Ge dimer upon the adsorption of H_2S. The calculated S-Ge bond length value for the most stable conformation (H_2S_{ad}) is 2.61 Å, and the two remaining S-H bond lengths are 1.35 and 1.38 Å. The strcutural parameters of other two conformations, H_2S_{ad}-1 and H_2S_{ad}-2, are similar to those of H_2S_{ad}. Figure 3 shows the DOS of surface Ge down atom and H_2S molecule before and after adsorption on Ge(100) surface, respectively. It is noticed from this figure that the H_2S molecule possesses C_{2v} symmetry with four valence states labled as $4a_1$, $2b_2$, $5a_1$, and $2b_1$ according to their orbital symmetries. These results are similar to that of our previous study.[32] The partial DOS (see Figure S1 of Supplementary information) indicates that states $4a_1$ and $2b_1$ are contributed mainly from 3s and $3p_z$ of S atom and $2b_2$ and $5a_1$ states arise from the hybridization of orbitals $3p_x$ and $3p_y$ of the S atom. All S 3p atomic orbitals ($2b_2$, $5a_1$, and $2b_1$ states), especially $3p_x$ and $3p_y$ of adsorbed H_2S have good overlaps with d orbitals of the buckled-down Ge which is bonded to the H_2S molecule.

3.2.Reaction Mechanism of H_2S on Ge(100)

We consider the reaction pathway for adsorption of H_2S on Ge(100) surface analogous to our previous study of the adsorption of H_2S on Si(100).[32] The calculated structural parameters and relative energies of intermediates and final products are listed in Table 2. The reaction energies, reaction barriers, and calculated imaginary frequencies of transition state structures are summarized in Table 3. The corresponding structures of intermediates and final products are shown in Figure 4 and the top views of their corresponding transition state structures are shown in Figure S2 of Supplementary information. The potential energy diagram (PES) for the adsorption and dissociation of H_2S

on the Ge(100) surface are shown in Figure 5. According to the calculation, the possible reaction paths are summarized in the following scheme:

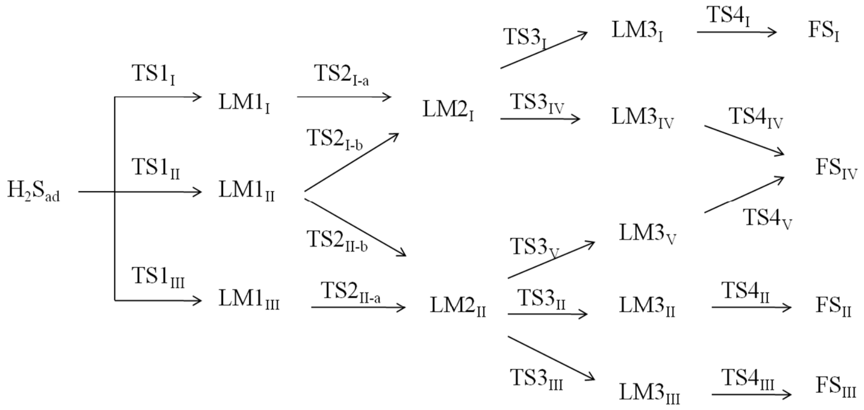

The possible reaction pathways described in above scheme includes first dehydrogenation, second dehydrogenation and sulfur bridged adsorption. The H_2S_{ad} species can undergo a first dehydrogenation through three paths. The first path is through $TS1_I$, with a 0.53 eV barrier, to produce $LM1_I$ intermediate; i.e., one H atom of H_2S dissociated and migrated to the Ge atom of an adjacent dimer along [001] direction. It has been observed that the first dehydrogenation has higher energy barrier due to the H atom being adsorbed on the Ge(3) atom. The second path creates the intermediate $LM1_{II}$ via $TS1_{II}$ with a barrier of 0.49 eV; i.e., the dissociated H and HS separately adsorb on each of a dimer's Ge atom. The third path yields intermediate $LM1_{III}$ via $TS1_{III}$ with the smallest barrier 0.10 eV; the resulting H and HS adsorb on Ge atoms of adjacent dimers along direction [010]. Figures 6(a) and (b) show the EDD contour plots which contain the dimeric S-Ge(1) bond with S-H_a and S-Ge (1) bond with S-H_b bond, respectively. It can be seen from Figure 6(a) that the electron density increases between the S and Ge(1) atoms which is bonded to H_2S, indicating a strengthening of S-Ge bond. In the meanwhile, the increased electron density is observed between the H and Ge(5) atoms of a neighboring Ge dimer along [010] direction (Figure 6(a)) which interacts with each other through a hydrogen bond. This interaction results in the lower energy barrier (0.10 eV) in the first dehydrogenation for H_2S_{ad} to form $LM1_{III}$. As summarized in Table 3, the reaction energies of the first dehydrogenations for the three paths are -0.89, -1.03, and -0.96 eV, respectively. $LM1_{II}$ and $LM1_{III}$ are comparably stable because the first dissociated H preferably adsorbs on the electron rich atoms like Ge(2) and Ge(5) atoms. The S-Ge bond length in $LM1_{I}$, $LM1_{II}$, and $LM1_{III}$ are shortened by ~0.3Å, compared to that of in the H_2S_{ad}. In H_2S_{ad}, H_2S adsorbed on a Ge atom via a dative bond; whereas in $LM1_{I\sim III}$, it is adsorbed on a Ge atom via a covalent bond.

Further, the local minima's $LM1_{I}$, and $LM1_{II}$ can undergo dehydrogenation and form $LM2_{I}$ via the transition states, $TS2_{I-a}$ and $TS2_{I-b}$ with energy barriers of 0.90 and 0.88 eV, respectively. $LM2_{II}$ can be produced from the dehydrogenation of $LM1_{III}$ and $LM1_{II}$ via transition states, $TS2_{II-a}$, and $TS2_{II-b}$ with barriers of 1.89 and 1.07 eV, respectively. From Table 2, it has been observed that the structural parameters of $LM2_{I}$ and $LM2_{II}$ are almost similar. The S-Ge bond of LM2 species is much shorter than that of LM1, indicating a stronger S-Ge bond in species LM2. The energy barriers of the second dehydrogenation, LM1→LM2, are higher than that of first dehydrogenation H_2S_{ad}→LM1. In the reaction mechanism, there are two types of intermediates between the LM2 and the final products; one is formed through the migration of H atom from $LM2_{I}$/$LM2_{II}$ ($LM3_{I}$, $LM3_{II}$ and $LM3_{III}$) and another one is formed through the bridging of two Ge dimer atoms via S adatom ($LM3_{IV}$ and $LM3_{V}$). In the first type, the transition states $TS3_{I}$, $TS3_{II}$, and $TS3_{III}$ are having the energy barriers of 1.26, 1.71, and 1.24 eV, respectively between the $LM2_{I\sim II}$ and $LM3_{I\sim III}$. Also, the S adatom remains bonded with Ge atom and has a dangling bond in $LM3_{I\sim III}$. The final products, $FS_{I\sim III}$ are formed from $LM3_{I\sim III}$ via $TS4_{I\sim III}$ with respective energy barriers of 0.48, 1.20, and 0.58 eV. $LM3_{I\sim III}$ can further transform with small barriers to the final products, $FS_{I\sim III}$. In FS_{I-III}, the S adatom bridges either two neighboring dimers along [001] direction or two Ge atoms of a dimer or two neighboring dimers along [010] direction, respectively. In $LM3_{IV}$ and $LM3_V$, the S adatom bridges two Ge atoms of a dimer (Figures 4i and 4j) and their formation barriers by corresponding transition states, $TS3_{IV}$ and $TS3_V$ are 0.47 eV and 0.30 eV, respectively. Further, $LM3_{IV}$ and $LM3_V$ isomerized to form the final product FS_{IV} (Figure 4n), with high barriers (1.13 and 1.43 eV, respectively. From Table 2, it has been noticed that the dimeric Ge-Ge bond length remains nearly at 2.56 ± 0.06 Å in all the intermediates and final products, except $LM3_{IV}$, $LM3_V$, FS_I and FS_{IV}. In the FS_I, the Ge(1)-Ge(2) bond length increases to 2.74Å because the Ge-S-Ge has ring stress. Also, the Ge(1)-Ge(2) bond is cleaved in $LM3_{IV}$, $LM3_V$ and FS_{IV}, so the bond length increases to 3.5Å~3.8Å.

There are four reaction paths for the dissociation of H_2S on Ge(100) surface are proposed and they are; $H_2S_{ad} \rightarrow LM1_I/LM1_{II} \rightarrow LM2_I \rightarrow LM3_I \rightarrow FS_I$, $H_2S_{ad} \rightarrow LM1_{II}/LM1_{III} \rightarrow LM2_{II} \rightarrow LM3_{II} \rightarrow FS_{II}$, $H_2S_{ad} \rightarrow LM1_{II}/LM1_{III} \rightarrow LM2_{II} \rightarrow LM3_{III} \rightarrow FS_{III}$, and $H_2S_{ad} \rightarrow LM1_{II} \rightarrow LM2_I/LM2_{II} \rightarrow LM3_{IV}/LM3_V \rightarrow FS_{IV}$. However from the calculated results of the rate-determining steps (RDS) for the final products (FS_I, FS_{II}, FS_{III} and $FS_{IV)}$ are $LM2_I \rightarrow LM3_{I,}$ $LM2_{II} \rightarrow LM3_{II}$, $LM2_{II} \rightarrow LM3_{III}$ and $LM3_V \rightarrow FS_{IV,}$ respectively. Their barriers at the rate-determining step are 1.26, 1.71, 1.24 and 1.43 eV, respectively. Among the four, the third RDS has the lowest energy barrier. According to these calculations, FS_{III} is thermodynamically more stable than the others and hence it can be the major product. The more ring strains in FS_I and FS_{IV} due to their inter- or intra- dimer lead to break the dimer bonds, so they are unstable products among the others.[23] From the above, it has been noticed that the final product FS_{III} is favorable in terms of both kinetic and thermodynamic points.

From Table 1, it has been found that the calcualted adsorption energy values for three possible adsorption conformations of H_2S on Ge(100) surface are smaller than that of

Si(100) surface. When H_2S adsorbs on surface, the 3p orbitals ($2b_2$, $5a_1$, and $2b_1$) of S atom have more significant overlap with p orbitals of buckled-down Si atom[32] than the d orbitals of buckled-down Ge atom. The strong overlap between the p-orbitals of S and Si atoms result in the large adsorption energies for the adsorption of H_2S_{ad} on Si(100) surface.[32] From Table 2, it is noticed that the relative energies for all the intermediates and final products of adsrotpion of H_2S on Si(100) surface are more negative than those on Ge(100) surface, which indicates that those are more stable on the Si surface. Based on the present and previous studies,[32] we summarized the total reaction energies for final products, energy barriers for RDS and RDS pathways from H_2S adsorbed on Ge or Si surface and are shown in Table 4. As can be seen from this table, FS_{II} and FS_{III} are thermodynamically favourable products for the H_2S adsorption on Ge(100) and Si(100), respectively. Their RDSs are from LM2 to LM3 via second dehydrogenation process. In the kinetic point of view, FS_I and FS_{IV} are the favorable products for Si surface and FS_I and FS_{III} are the major prodcuts for Ge surface. From the above results, it is noted that the final prodcut FS_{III} is thermodynamically and kinetically favorable product for the H_2S adsorption on Ge surface. From the above results it has been observed that the S-passivation products on Si(100) surface are more stable than Ge(100) surface.

3.3.Density of States (DOS)

The electronic structure is intimately related to their fundamental physical and chemical properties. To further understand the adsorption modes of H_2S on Ge(100), we analyzed DOS of most possible reaction pathway i.e., $H_2S_{ad}\rightarrow LM1_{II}\rightarrow LM2_{II}\rightarrow LM3_{III}\rightarrow FS_{III}$, which includes five different S conformations such as H_2S, HS, S adatom and bridged S atoms. The plotted DOS for H_2S_{ad}, $LM1_{II}$, $LM2_{II}$, $LM3_{III}$ and FS_{III} are shown in Figure 7 and it compares the different S conformations adsorbed on Ge(100) surface. In the Figure 7, the sharp band appears between -10 to -15 eV relative to the Fermi level is attributed from the

3s orbital of S atoms, which is adsorbed on the surface with different configurations. Initially, when the H_2S species absorbs on the Ge(100) surface, this band located at-15.86 eV region (Figure 7a.) and the first and second dehydrogenation shifts this band towards the Fermi level (from -15.86 to -13.5/-11.8 eV, see Figures 7b and 7c). This upward shift can be explained that the interaction of H_2S on the surface via dative bond, whereas after the first dehydrogenation, $LM1_{II}$ species interact with surface via single bond. Also, the peak at -8.2 eV region (Figure 7a) is due to the p_x orbital of S atom shifts close to the Fermi level after the first dehydrogenation and finally it overlaps with the p_y and pz orbitals after the second dehydrogenation, which is due to the interaction of S atom with the surface by either dative bond or covalent bond. In $LM2_{II}$ and $LM3_{III}$, S atom adsorbed in a similar way and hence, the PDOS for adsorbed S atom resembles same (at -11.89 and -12.67 eV respectively in Figure 7c and d). Finally, the FS_{III} possesses bridged S conformation on Ge(100) surface, so its 3s orbital band shifted downward and close to the HS conformation. Also, the broad band in the region of 0 to -5 eV, shows the bonding interaction of p orbitals of S and Ge surface atoms. These above results demonstrate that DOS spectra can comprehensively explain the interaction of adsorbed S atom and surface Ge atom

3.4.Vibrational Frequency Analysis for H_2S Adsorption on Ge(100)

In order to guide a future surface vibrational spectroscopic study, the vibrational frequencies for adsorbed species on Ge(100) surface are analyzed. The calculated vibrational frequencies for the adsorbed species such as, H_2S, LM, and FS species are summarized in Table 5. The bands observed at 2577 and 2159 cm^{-1} for H_2S species are due to asymmetric and symmetric S-H stretching modes. The strong interaction between H_b and Ge (5) atoms (see Figure 6) leads to weaken the S-H_b bond resulted in redshift of wave number for S-H stretching mode (2159 cm^{-1}). The H-Ge stretching bands are observed in the range of 1900-2024 cm^{-1}. The calculated S-H and H-Ge stretching modes of $LM1_{II}$ are in agreement with the previous EELS experimental values of 2532cm^{-1} and 1967 cm^{-1}.[37] For S-Ge stretching bands, LM1$_{I\sim III}$ belong to the first dissociated group which display similar S-Ge stretching vibration on the surface. There is about 80 cm^{-1} difference between the H_2S_{ad} and LM1$_{I\sim III}$ for S-Ge stretching mode, which is due to the change in interaction type, i.e. from dative bond to covalent bond between sulfur atom and Ge surface. The other dissociated intermediates (LM2$_{I\sim II}$ and LM3$_{I\sim III}$) exhibits blue shift in the IR spectrum, which is due to the increase in the bond order of S-Ge after the second dehydrogenation. The S-Ge stretching bands for LM3$_{IV\text{-}V}$ and FS$_{I\text{-}IV}$ are observed at about 300-420cm^{-1} which is red shifted due to the interaction of bridged sulfur atom with the Ge atom via covalent bond. As shown in Table 5, the calculated S-Ge vibration frequencies of FS$_I$ are red shifted (about 50 to 130 cm^{-1}) compared to other final products, which indicates that the bond of dimeric Ge become longer because of the ring stress from the Ge-S-Ge bonds.

4. Conclusions

We have performed the detailed investigation of the adsorption and dissociation of H_2S on Ge(100) surface using density functional theory calculations. Our results show that among the three different conformation, H_2S_{ad} is found to be adsorbed stably on the surface. Possible reaction paths are proposed for dehydrogenation between adsorbed H_2S and S adatoms. In the first step, adsorbed H_2S partially dissociates and produced HS and H and in the second step, HS further dissociates into S adatom. Further, the EDD contour indicate that the increased electron density between the H atom and Ge(5) atom of a neighboring Ge dimer along [010] which leads to the lower energy barrier (0.10 eV) in the first dehydrogenation for H_2S_{ad} to $LM1_{III}$. The results show that the four final products have more stable conformations via LM1, LM2, and LM3 intermediates. We found that FS_I and FS_{III} are kinetically favored products whereas FS_{II} and FS_{III} are thermodynamically favored products for the H_2S adsorption on the Ge surface. In addition, the interactions between S and Ge atoms are identified by DOS spectra. The calculated results of IR spectra are in good agreement with the available experimental EELS data.

Acknowledgments. National Science Council of Taiwan (NSC 96-2120-M-011-001 and NSC-97-2113-M-011-001) supported this research. We are also grateful to National Center of High-Performance Computing, Institute of Nuclear Energy Research, and Atomic Energy Council in Taiwan for their support.

Supplementary information Table S1 lists the lattice parameters of Ge obtained with various pseudopotentials. Table S2 displays dimer bond length (d_D) and dimer tilting angle (θ) for a clean Ge(100) surface, compared with results from other calculations and experimental data. Figure S1 illustrates the partial DOS of H_2S adsorbed on the Ge(100) surface. Figure S2 shows a top view of all transition structures on the reaction paths of adsorbed H_2S.

References:

1. K. Kita, K. Kyuno and A. Toriumi, *Appl Phys Lett*, 2004, 85, 52-54.
2. H. Kim, P. C. McIntyre, C. O. Chui, K. C. Saraswat and M. H. Cho, *Appl Phys Lett*, 2004, 85, 2902-2904.
3. A. Dimoulas, G. Mavrou, G. Vellianitis, E. Evangelou, N. Boukos, M. Houssa and M. Caymax, *Appl Phys Lett*, 2005, 86, 032908.
4. P. W. Loscutoff and S. F. Bent, *Annu Rev Phys Chem*, 2006, 57, 467-495.
5. D. Misra, R. Garg, P. Srinivasan, N. Rahim and N. A. Chowdhury, *Mat Sci Semicon Proc*, 2006, 9, 741-748.
6. K. Martens, B. De Jaeger, R. Bonzom, J. Van Steenbergen, M. Meuris, G. Groeseneken and H. Maes, *Ieee Electr Device L*, 2006, 27, 405-408.
7. N. Wu, Q. C. Zhang, C. X. Zhu, D. S. H. Chan, M. F. Li, N. Balasubramanian, A. Chin and D. L. Kwong, *Appl Phys Lett*, 2004, 85, 4127-4129.
8. G. W. Anderson, M. C. Hanf, P. R. Norton, Z. H. Lu and M. J. Graham, *Appl Phys Lett*, 1995, 66, 1123-1125.
9. L. M. Nelen, K. Fuller and C. M. Greenlief, *Appl Surf Sci*, 1999, 150, 65-72.
10. M. Houssa, G. Pourtois, B. Kaczer, B. De Jaeger, F. E. Leys, D. Nelis, K. Paredis, A. Vantomme, M. Caymax, M. Meuris and M. M. Heyns, *Microelectron Eng*, 2007, 84, 2267-2273.
11. D. R. Fitzgerald and D. J. Doren, *J Am Chem Soc*, 2000, 122, 12334-12339.
12. P. Kruger and J. Pollmann, *Phys Rev Lett*, 1995, 74, 1155-1158.
13. T. Shirasawa, S. Mizuno and H. Tochihara, *Surf Sci*, 2006, 600, 815-819.
14. C. Yang and H. C. Kang, *J Chem Phys*, 1999, 110, 11029-11037.
15. J. A. Kubby and J. J. Boland, *Surf Sci Rep*, 1996, 26, 61-204.
16. T. Weser, A. Bogen, B. Konrad, R. D. Schnell, C. A. Schug, Steinmann and W, *Phys Rev B*, 1987, 35, 8184-8188.
17. M. Gothelid, G. LeLay, C. Wigren, M. Bjorkqvist, M. Rad and U. O. Karlsson, *Appl Surf Sci*, 1997, 115, 87-95.
18. M. Cakmak and G. P. Srivastava, *Phys Rev B*, 1999, 60, 5497-5505.
19. C. Fleischmann, S. Sioncke, S. Couet, K. Schouteden, B. Beckhoff, M. Muller, P. Honicke, M. Kolbe, C. Van Haesendonck, M. Meuris, K. Temst and A. Vantomme, *J Electrochem Soc*, 2011, 158, H589-H594.
20. C. Fleischmann, M. Houssa, M. Muller, B. Beckhoff, H. G. Boyen, M. Meuris, K. Temst and A. Vantomme, *J Phys Chem C*, 2013, 117, 7451-7458.
21. H. J. Kuhr and W. Ranke, *Surf Sci*, 1987, 189–190, 420-425.
22. D. Lee, K. Kubo, T. Kanashima and M. Okuyama, *Jpn J Appl Phys*, 2012, 51.
23. T.-F. Teng, W.-L. Lee, Y.-F. Chang, J.-C. Jiang, J.-H. Wang and W.-H. Hung, *J Phys Chem C*, 2009, 114, 1019-1027.
24. S. Sioncke, J. Ceuppens, D. Lin, L. Nyns, A. Delabie, H. Struyf, S. De Gendt, M. Muller, B. Beckhoff and M. Caymax, *Microelectron Eng*, 2011, 88, 1553-1556.
25. J. S. Kachian and S. F. Bent, *J Am Chem Soc*, 2009, 131, 7005-7015.
26. G. Kresse and J. Furthmuller, *Comp Mater Sci*, 1996, 6, 15-50.
27. G. Kresse and J. Hafner, *Phys Rev B*, 1993, 48, 13115-13118.
28. G. Kresse and J. Furthmüller, *Phys Rev B*, 1996, 54, 11169-11186.
29. D. Vanderbilt, *Phys Rev B*, 1990, 41, 7892-7895.
30. G. Henkelman, B. P. Uberuaga and H. Jonsson, *J Chem Phys*, 2000, 113, 9901-9904.
31. G. Mills, H. Jonsson and G. K. Schenter, *Surf Sci*, 1995, 324, 305-337.
32. T. F. Teng, C. Y. Chou, W. H. Hung and J. C. Jiang, *J Phys Chem C*, 2011, 115, 19203-19209.
33. Z. G. Wang, X. T. Zu, J. L. Nie and H. Y. Xiao, *Chem Phys*, 2006, 325, 525-530.

34. P. Krüger and J. Pollmann, *Appl. Phys. A*, 1994, 59, 487-502.
35. R. Rossmann, H. L. Meyerheim, V. Jahns, J. Wever, W. Moritz, D. Wolf, D. Dornisch and H. Schulz, *Surf Sci*, 1992, 199-209.
36. S. Hong, Y. E. Cho, J. Y. Maeng and S. Kim, *J Phys Chem B*, 2004, 108, 15229-15232.
37. K. T. Leung, L. J. Terminello, Z. Hussain, X. S. Zhang, T. Hayashi and D. A. Shirley, *Phys Rev B*, 1988, 38, 8241-8248.

Table 1. The calculated structural parameters and adsorption energies (E_{ads}) for hydrogen sulphide (H_2S) adsorption on Ge(100) surface.

System	*d*(S-H) (Å)	*d*(S-Ge) (Å)	*d*(Ge-Ge) (Å)	∠HSH (deg)	Ge-Ge tilting angle (deg)	E_{ads} (eV)	$^{a}E_{ads}$ (eV)
H_2S_{ad}	1.35/1.38	2.61	2.58	92.4	16	-0.49	-0.74
H_2S_{ad}-1	1.35/1.37	2.64	2.58	91.9	17	-0.40	-0.70
H_2S_{ad}-2	1.33/1.39	2.63	2.57	92.5	16	-0.30	-0.65

[a] The calcualted adsorption energy for H_2S adsorption on Si(100) surface taken from previous study.[32]

Table 2. The calculated structural parameters and relative energies for dissociatively adsorbed H_2S on Ge(100) surface.

Local minima and final products	***d*(Ge-Ge)[a] (Å)**	***d*(Ge-Ge)[b] (Å)**	***d*(S-Ge) (Å)**	***d*(H-Ge) (Å)**	***E*rel (eV)[d]**
LM1$_{I}$	2.55	2.58	2.28	1.57	−0.89(−0.95)
LM1$_{II}$	2.51 (2.46[c])	2.51 (2.46[c])	2.28 (2.18[c])	1.55 (1.56[c])	−1.03(−1.43)
LM1$_{III}$	2.60	2.53	2.29	1.54	−0.96(−1.31)
LM2$_{I}$	2.52	2.58	2.10	1.55	−0.67(−1.05)
LM2$_{II}$	2.52	2.54	2.11	1.55	−0.67(−1.33)
LM3$_{I}$	2.56	2.59	2.11	1.55	−0.16(−1.13)
LM3$_{II}$	2.62	2.48	2.12	1.54	−1.03(−1.45)
LM3$_{III}$	2.54	2.58	2.11	1.56	−1.19(−1.45)
LM3$_{IV}$	3.88	2.57	2.24/2.33	1.55	−0.88(−1.46)
LM3$_{V}$	3.45	2.55	2.21/2.34	1.55	−1.12(−1.59)
FS$_{I}$	2.74	2.73	2.36	1.56	−0.81(−1.38)
FS$_{II}$	2.52	2.47	2.17 (2.16[c])	1.54 (1.56[c])	−1.27(−2.63)
FS$_{III}$	2.51	2.53	2.33	1.55	−1.34(−2.12)
FS$_{IV}$	3.56	-	2.25/2.28	1.55	−1.21(−1.99)

[a] Bond length of a Ge(1)-Ge(2) dimer which is bonded either with HS or S.

[b] Bond length of a Ge(3)-Ge(4) or Ge(5)-Ge(6) which is bonded with dissociative H.

[c] Taken from Reference[18]

[d] Relative energy for H_2S on Si(100) surface are given in parenthesis.

Table 3: The calculated reaction barriers ($^{\ddagger}E$, eV), reaction energies (ΔE, eV), and imaginary frequencies (IMF, cm^{-1}) for the transition states of decomposition of H_2S on Ge(100) Surface.

Reaction Path	$^{\ddagger}E$	ΔE	**IMF**
$H_2S_{ad} \rightarrow TS1_{I} \rightarrow LM1_{I}$	0.53	-0.89	227*i*
$H_2S_{ad} \rightarrow TS1_{II} \rightarrow LM1_{II}$	0.49	-1.03	661*i*
$H_2S_{ad} \rightarrow TS1_{III} \rightarrow LM1_{III}$	0.10	-0.96	300*i*
$LM1_{I} \rightarrow TS2_{I\text{-}a} \rightarrow LM2_{I}$	0.90	0.22	492*i*
$LM1_{II} \rightarrow TS2_{I\text{-}b} \rightarrow LM2_{I}$	0.88	0.36	419*i*
$LM1_{III} \rightarrow TS2_{II\text{-}a} \rightarrow LM2_{II}$	1.89	0.29	1029*i*
$LM1_{II} \rightarrow TS2_{II\text{-}b} \rightarrow LM2_{II}$	1.07	0.36	421*i*
$LM2_{I} \rightarrow TS3_{I} \rightarrow LM3_{I}$	1.26	0.51	552*i*
$LM2_{II} \rightarrow TS3_{II} \rightarrow LM3_{II}$	1.71	-0.36	405*i*
$LM2_{II} \rightarrow TS3_{III} \rightarrow LM3_{III}$	1.24	-0.52	274*i*
$LM2_{I} \rightarrow TS3_{IV} \rightarrow LM3_{IV}$	0.47	-0.32	128*i*
$LM2_{II} \rightarrow TS3_{V} \rightarrow LM3_{V}$	0.30	-0.46	197*i*
$LM3_{I} \rightarrow TS4_{I} \rightarrow FS_{I}$	0.48	-0.65	145*i*
$LM3_{II} \rightarrow TS4_{II} \rightarrow FS_{II}$	1.20	-0.10	119*i*
$LM3_{III} \rightarrow TS4_{III} \rightarrow FS_{III}$	0.58	-0.01	162*i*
$LM3_{IV} \rightarrow TS4_{IV} \rightarrow FS_{IV}$	1.13	-0.22	919*i*
$LM3_{V} \rightarrow TS4_{V} \rightarrow FS_{IV}$	1.43	-0.09	347*i*

Table 4. The calculated total reaction energies (ΔE in eV) for the final products, energy barrier (‡E in eV) for RDSs and their corresponding pathways for the adsorption of H_2S on Ge and Si surface.

Final Products	**ΔE**		**‡E**		**RDS**	
	Ge	**Si**	**Ge**	**Si**	**Ge**	**Si**
FS_I	-0.81	-1.38	1.26	1.19	$LM2_I \rightarrow LM3_I$	$LM2_I \rightarrow LM3_I$
FS_{II}	-1.27	-2.63	1.71	1.63	$LM2_{II} \rightarrow LM3_{II}$	$LM2_{II} \rightarrow LM3_{II}$
FS_{III}	-1.34	-2.12	1.24	1.54	$LM2_{II} \rightarrow LM3_{III}$	$LM2_{II} \rightarrow LM3_{III}$
FS_{IV}	-1.21	-1.99	1.43	1.22	$LM3_V \rightarrow FS_{IV}$	$LM3_V \rightarrow FS_{IV}$

Table 5: The calculated vibrational frequencies of the initial state (H_2S_{ad}), local minima's (LM), and final products (FS) for the decomposition of H_2S on Ge(100) Surfaces.

System	**ν H-S (cm^{-1})**	**ν H-Ge (cm^{-1})**	**ν S-Ge (cm^{-1})**
H_2S_{ad}	2577/2159		265
$LM1_I$	2600	1926	342
$LM1_{II}$	2544	1967	331
$LM1_{III}$	2389	2024	348
$LM2_I$		1962/1915	456
$LM2_{II}$		1979/1968	461
$LM3_I$		1970/1921	463
$LM3_{II}$		2000/1968	448
$LM3_{III}$		1948/1927	450
$LM3_{IV}$		1913/1908	351/310
$LM3_V$		1934/1916	364/295
FS_I		1914/1903	291/282
FS_{II}		1998/1994	421/267
FS_{III}		1991/1983	344/276
FS_{IV}		1951/1923	396/333

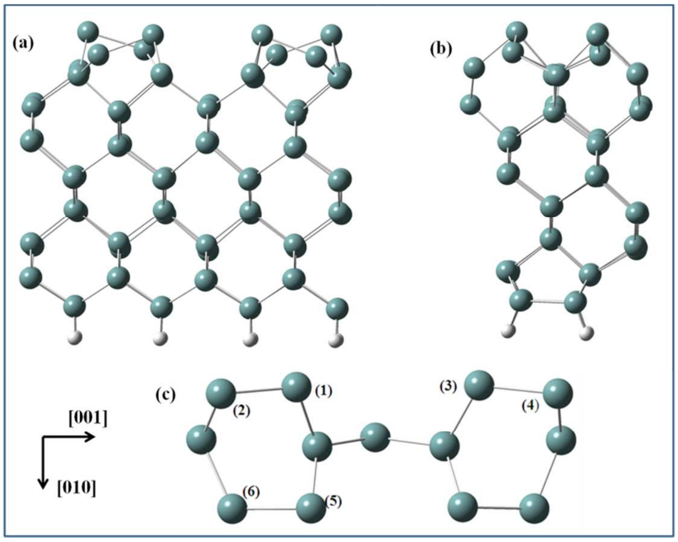

Figure 1. The optimized structure of Ge(100)-c(4x2) surface: (a) front view, (b) side view and (c) top view.

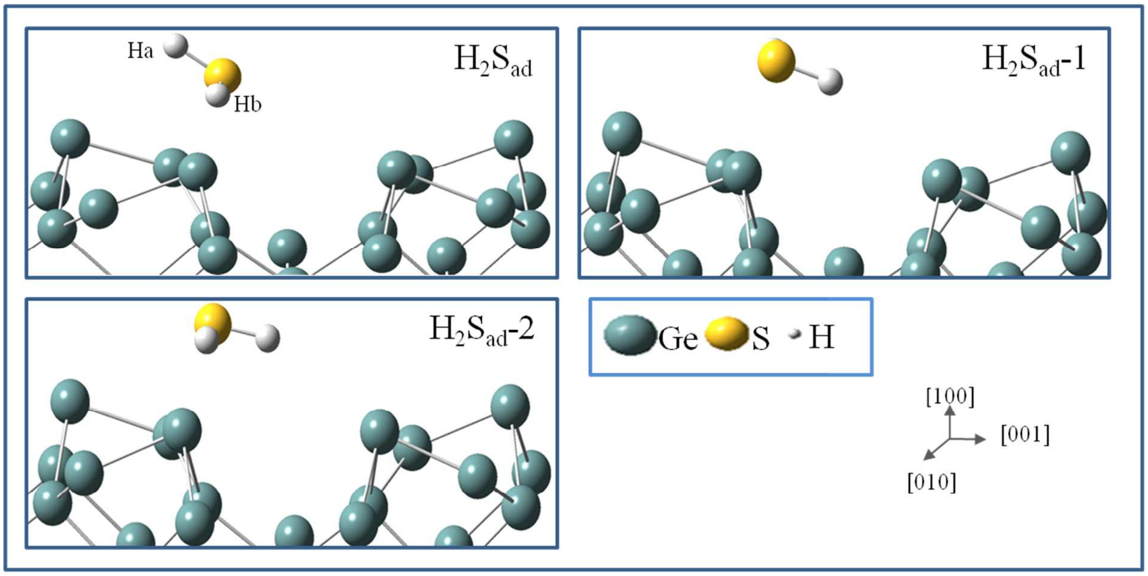

Figure 2. The optimized structures of different conformations of H_2S adsorbed on Ge(100) surface: (a) H_2S_{ad}, (b) H_2S_{ad}-1, and (c) H_2S_{ad}-2.

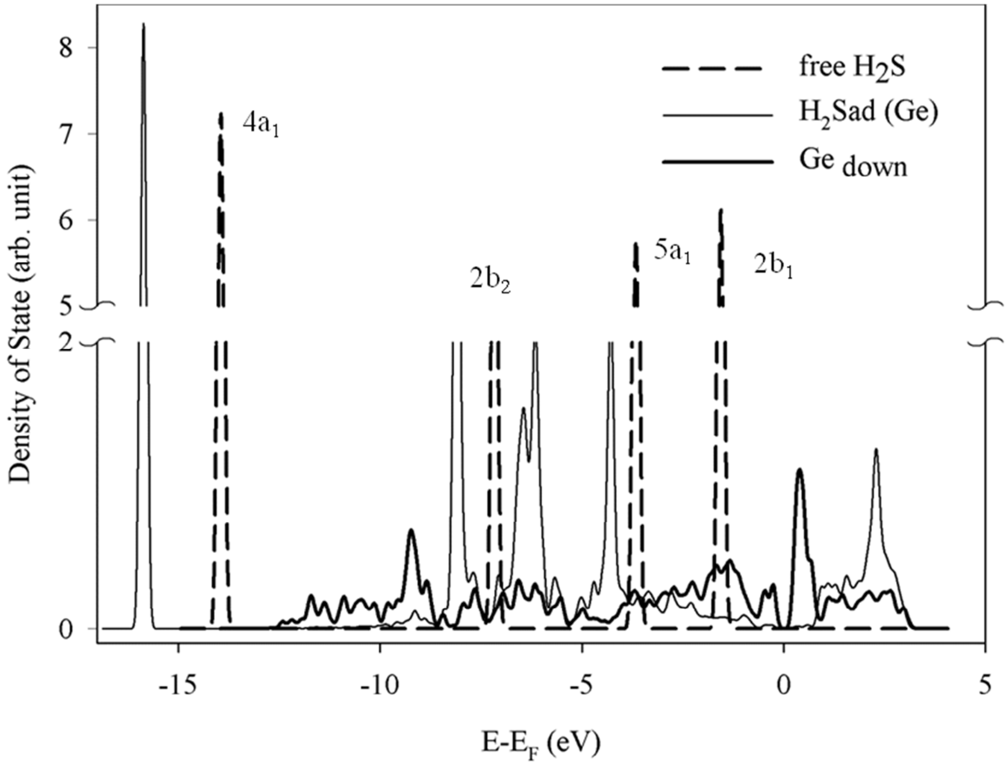

Figure 3. The DOS of a H_2S molecule before (dashed line) and after (black solid line) adsorption on Ge (100) and DOS of Ge down atom (bond black line) bonded with H_2S.

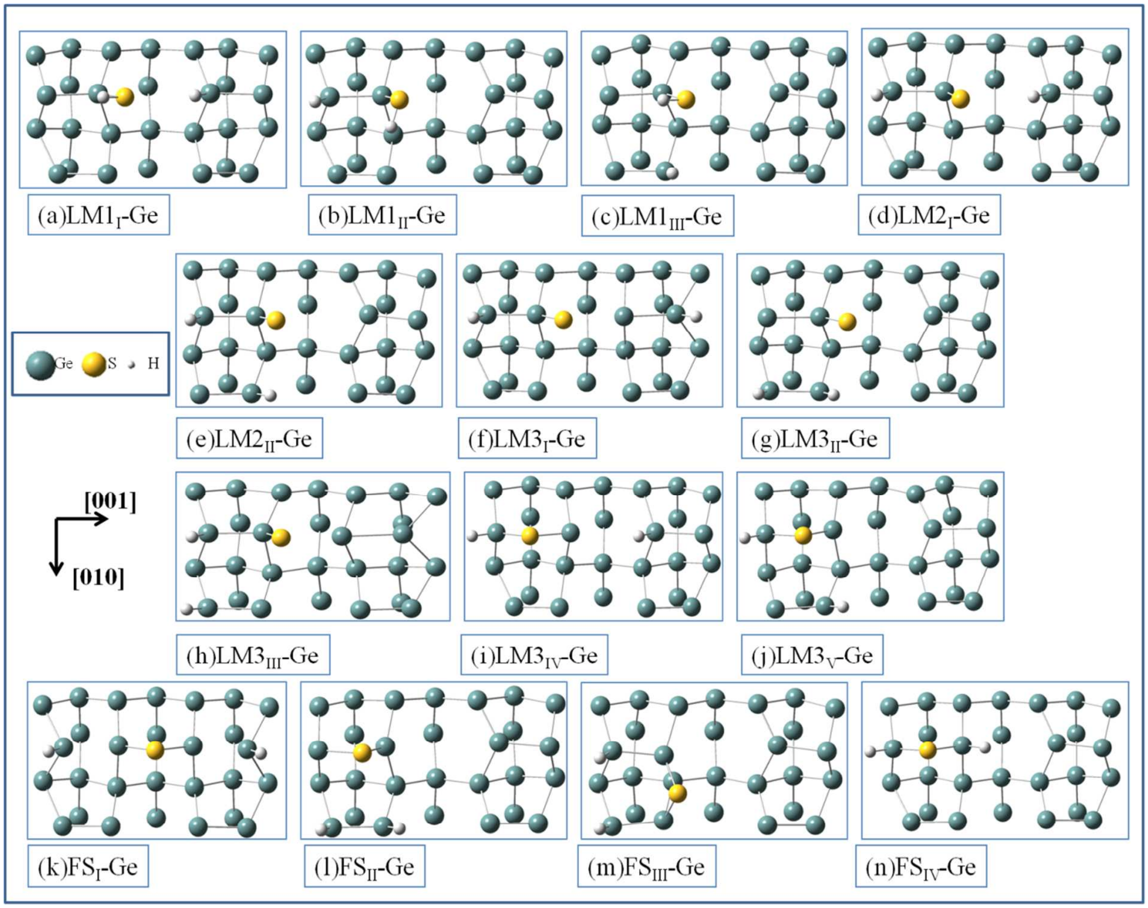

Figure 4. Top view of all the local minima's and the final products of the reactions for the adsorption of H_2S on Ge(100) surface.

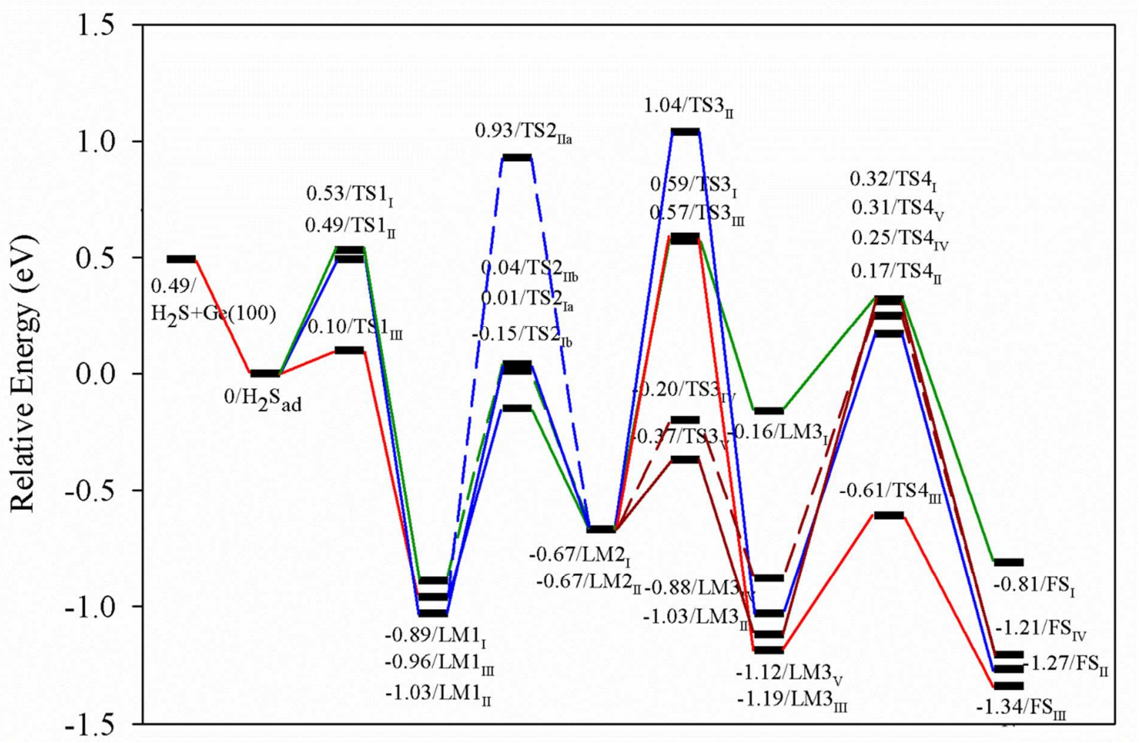

Figure 5. Potential-energy diagram for adsorption and decomposition of H_2S on Ge(100) surface. All potential energies of intermediates, transition structures, and final products are referred to the H_2S molecule adsorbed on the surface.

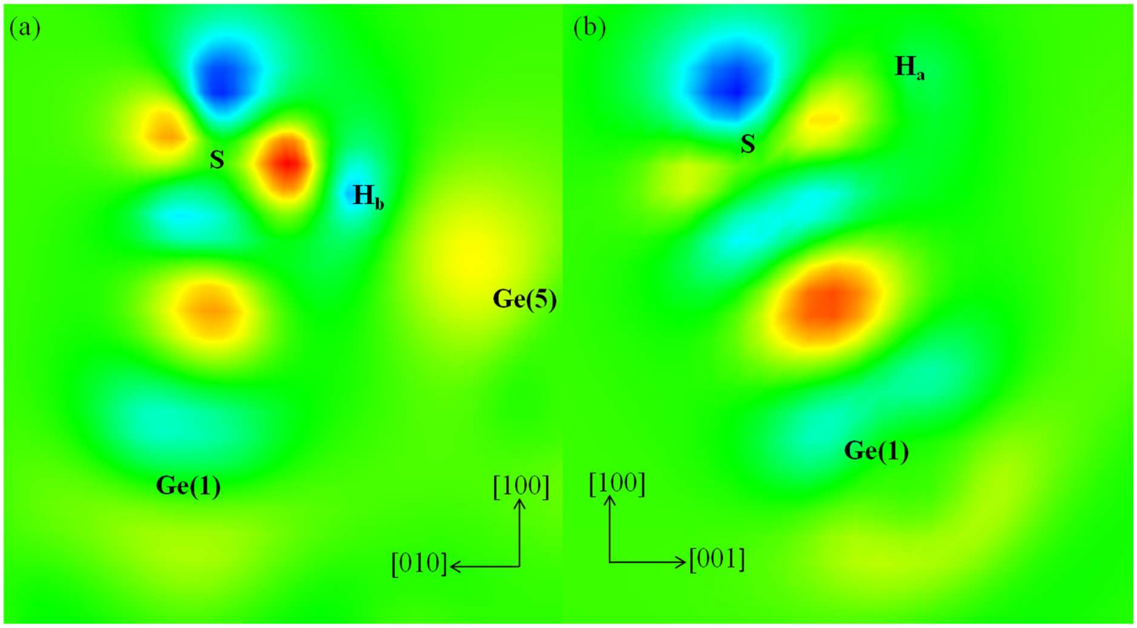

Figure 6. EDD contours of H_2S_{ad} on a plane containing (a) a S-Ge(1) bond and a dimeric S-H_a bond along [010] and (b) a S-Ge(1) bond and a dimeric S-H_b bond along [001]. The red and blue colors represent the increasing and decreasing electron densities, respectively.

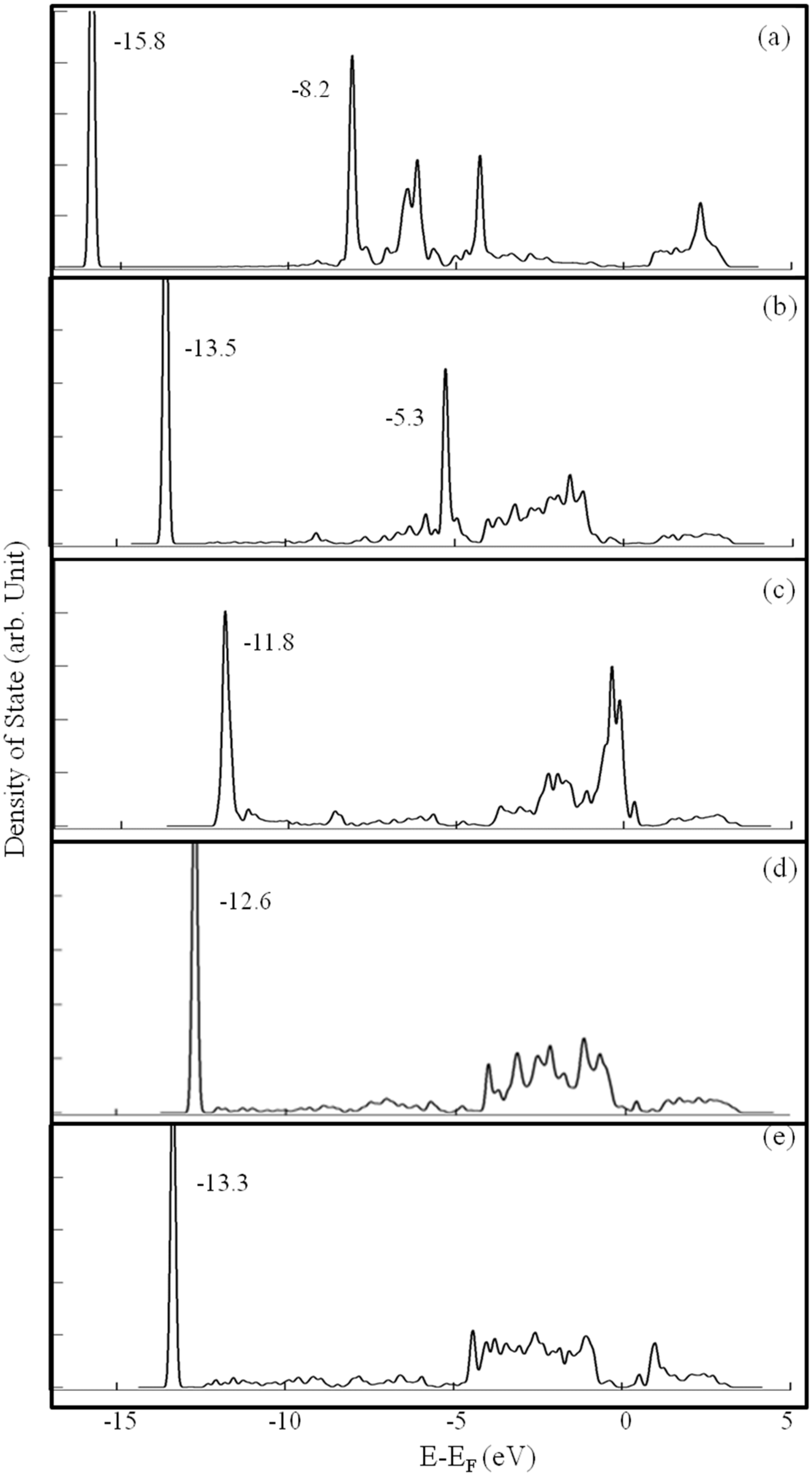

Figure 7. The total DOS of S adatom in (a) H_2S_{ad}, (b) $LM1_{II}$, (c) $LM2_{II}$, (d) $LM3_{III}$, and (e) FS_{III} structures.

TOC